

## THE SENSITIVITY OF A 3D STREET CANYON CFD MODEL TO UNCERTAINTIES IN INPUT PARAMETERS.

*James F. Benson, Nick Dixon, Tilo Ziehn and Alison S. Tomlin*  
Energy and Resources Research Institute (ERRI), University of Leeds, UK

### INTRODUCTION

Although much progress has been made in the development of three dimensional computational fluid dynamic (CFD) models of turbulent flows in urban streets, their evaluation with respect to relevant field and laboratory data is less common. Since the models usually include parameterisations of some important features, their evaluation benefits from the inclusion of sensitivity studies that highlight the impact of uncertain input parameters on predicted flow fields. It is fair to say that using current resources, operational CFD models are more likely to employ a RANS (Reynolds Average Navier Stokes) approach than more computationally expensive eddy-resolving models such as Large Eddy Simulation (LES). However, in order to model the flow and turbulence within complex geometries, a RANS model needs to make many assumptions. Close to a surface the turbulence needs to be modelled using boundary conditions that reflect the surface roughness. For many *k-e* models these boundary conditions use an idealised empirical relationship known as the log law. This assumes that the boundary grid point is within a region that has conditions similar to that used to derive the log law, such as a logarithmic velocity profile and constant shear stress. This assumption may not be true over urban areas where the surface is non-homogeneous and wind profiles are a result of the interaction of the background flow with many different surface types. Apart from the uncertainties due to the input parameters, the model physics may be based upon assumptions that are not correct in many situations, such as using isotropic eddy viscosity in *k-e* models. Overall model evaluation should therefore also contain elements of comparison with measured results. This paper presents both uncertainty and sensitivity analysis combined with comparisons to experimental results. A description of methods used in the evaluation of CFD models for urban-scale flow and dispersion studies has been referred to in the companion paper, Ziehn & Tomlin (2007). This paper aims to link the results of such sensitivity analysis to the physical aspects of the model behaviour.

### MODEL

The model used for this study is the *k-e* model MISKAM (Eichhorn, 1996) as introduced in Ziehn & Tomlin (2007). Dixon et al. (2006) provided a crude sensitivity analysis of MISKAM outputs to inflow roughness length, but a full global uncertainty and sensitivity analysis was not given, prohibiting the investigation of the sources of discrepancy between the modelled and experimentally measured flow field. The aim of this work is to explore whether the sources of such discrepancy can be attributed to parametric uncertainties in the main inputs of the model, or imply problems within the description of the model equations.

The model consists of 3D RANS equations, with wall boundaries using the law of the wall (1) and a no slip condition (i.e. zero velocity at the wall):

$$u = \frac{u_*}{\mathbf{k}} \ln \left( \frac{z + z_0}{z_0} \right) \quad (1),$$

where  $z_0$  is the surface roughness length,  $u_*$  is the friction velocity,  $z$  is height above a surface and  $\mathbf{k}$  is the Von Karman constant. One difference from the standard law of the wall is that (1) uses  $z+z_0$  instead of simply  $z$ . This is because if the height of the first grid point is the same as the roughness length then the log law cannot be applied. As the log law requires constant

Reynolds stresses for its derivation, equilibrium between turbulent kinetic energy (TKE) production and dissipation is assumed. At the boundary grid point,  $k$  and  $e$  are found using:

$$k = \frac{u_*^2}{\sqrt{C_m}} \quad (2),$$

$$e = \frac{u_*^3}{k_z} \quad (3)$$

combined with (1), where  $C_\mu=0.09$ . MISKAM initialises with a one-dimensional inflow profile. This is calculated using the inflow surface roughness length to calculate bottom boundary grid point  $k$  and  $e$  values using (1)-(3). The  $k$ - $e$  model is then iteratively solved in one-dimension to give velocity, TKE, and dissipation inflow profiles. This 1D profile is initially applied horizontally across the entire model domain. Boundary values of  $k$  (2) and  $e$  (3) can now be calculated for all surfaces, followed by  $k$  and  $e$  equations being solved across the entire model domain. This is followed by calculation of wind components. The resulting outputs represent time averaged quantities.

## MODEL SCENARIO

The location modelled in this study is that of Gillygate, York, the site of an extensive measurement campaign (Boddy et al., 2005a, 2005b) that provides observations which can be compared to the output of the MISKAM model. A full description of the model scenario was given in the companion paper Ziehn & Tomlin (2007). Gillygate is a narrow street canyon of width ~15m with two and three storey buildings on each side of typical height 10-12m. There are two measurement points, G3 and G4, allowing comparison of full scale measurement results with the model output. They are situated at heights of 5.5m (G3) and 5.7m (G4). G3 is 2m from the wall while G4 is only 1m from the wall. The cross sections presented in this paper are taken across the  $x$ - $z$  plane intersecting G3 and G4 ( $y=211$ m). Background wind was measured at a mast location at a height of 19.5m.

## SENSITIVITY ANALYSIS

Sensitivity analysis shows how a model output changes according to the model inputs. Thus the overall uncertainty of the model may be associated with the individual uncertainty in each model input. Here, global methods based on random sampling Monte-Carlo techniques (RS-MC) and random sampling high dimensional model representations (RS-HDMR, Rabitz et al., 1999) have been used to perform uncertainty and sensitivity analysis. As demonstrated in Ziehn & Tomlin (2007), the HDMR method allows the calculation of each parameter's contribution to the overall output variance, based on its given range of input values.

As in Ziehn & Tomlin (2007) there are four main input parameters included in this sensitivity study of the MISKAM model. They are the surface roughness (0.5-50cm), inflow roughness (5-50cm), wall roughness (0.5-10cm) and background wind direction  $\mathbf{q} \pm 10^\circ$ . The input ranges chosen are indicated in the brackets.  $\mathbf{q}$  is varied in this study to show how large an effect miss-specifying a reference wind direction may have if comparing the model to full scale measurements. In practice this is likely to be an uncertain parameter since the background wind direction may be measured far away from the measurement site or may be obtained from a model forecast. The sensitivity index for  $\mathbf{q}$  will determine the effect of such practical limitations on the predicted model output. The random sampling Monte-Carlo method generated random samples from across the input parameter ranges. The model was then run repeatedly using each of these random samples. The HDMR method uses quasi random sampling (RS) as described in Ziehn & Tomlin, (2007) with 1024 model runs used for each

wind angle. The outputs examined in this paper are the TKE ( $\kappa$ ) and mean wind speed ( $U = \sqrt{u^2 + v^2 + w^2}$ ).

To obtain the contribution of each input parameter to the overall output uncertainty we compare both Pearson and Spearman ranked correlation coefficients from the RS-MC results to RS-HDMR sensitivity indices. By applying a linear regression fit to the output from the RS-MC method for a given input, the Pearson correlation coefficient can be calculated. Because the Pearson coefficient is only a measure of the linear response, the Spearman ranked correlation ( $r_{sp}$ ) method is also used. This allows the correlation of any monotonically varying output to be estimated. The square of the correlation coefficient ( $r^2$ ) is equivalent to the fraction of the total output variance explained by a first order linear effect for that parameter.

## RESULTS

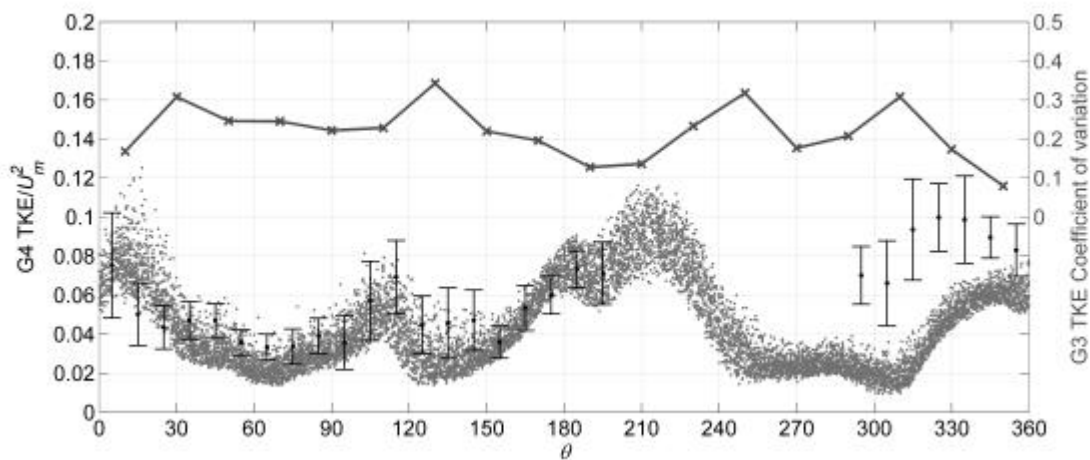


Fig. 1; G3 TKE/ $U_m^2$  experimental 15 minute averages in comparison with model results. The error bars on the experimental data are the standard deviations from the mean. Crosses - coefficient of variation for the model results.

Using 10000 runs across all  $\mathbf{q}$ , comparisons of model and full-scale experimental results at measurement point G3 are presented in Figure 1. The experimental data are 15 minute averages from the field campaign (Boddy et al., 2005a) grouped into 20° bins. The model data includes all the uncertainty in the model input parameters. For any particular  $\mathbf{q}$  the scatter around the mean can be considered the uncertainty in the models predictions due to the various roughness input parameter uncertainties. Taking these into account, the modelled TKE at G3 shows good agreement with the experimental results between 0 and 190 degrees (Figure 1). Due to the effect of the tree near the mast, the experimental data between 195 and 270 degrees is not shown (Dixon et al., 2006) since it affects the normalisation of the data. Figure 1 also shows that the model output variability is fairly small in comparison to the mean model output, since the coefficient of variation (standard deviation divided by mean) for all  $\mathbf{q}$  is below 0.4 at G3. The largest variations in normalised TKE are due to bulk changes in background wind direction  $\mathbf{q}$ . The choice of background wind angle range is therefore important when interpreting the results from the angle specific sensitivity tests. Its relative importance as an input parameter is expected to be dependant on its chosen range.

Table 1. Sensitivity of  $U$  at G3 to each parameter given by Pearson, Spearman ranked correlation coefficients and RS-HDMR first order sensitivity indices for  $\theta = 90 \pm 10^\circ$ .

	Pearson correlations		Spearman Ranked Correlations		HDMR first order
	r	r <sup>2</sup>	r <sub>sp</sub>	r <sub>sp</sub> <sup>2</sup>	
surface roughness	-0.4924	0.2424	-0.4917	0.2417	0.2833
wall roughness	-0.1846	0.0341	-0.1968	0.0387	0.0491
inflow roughness	-0.1747	0.0305	-0.1651	0.0273	0.0359
wind direction ( $q$ )	-0.7610	0.5791	-0.7570	0.5731	0.6438
total		0.8861		0.8808	1.0121

Table 1 shows the sensitivity of  $U$  at G3 to each input parameter for  $q = 90 \pm 10^\circ$ . The differences in the sensitivity results using the Pearson and Spearman correlation coefficients compared to the HDMR 1<sup>st</sup> order sensitivity indices can be explained by the nonlinearity in the output response. The HMDR method gives a more accurate representation of the overall response to the input parameter than either of the two correlation methods across the whole input range. Since the 1<sup>st</sup> order sensitivity indices sum to almost 1, this suggests that the responses to parameter changes for this output are nonlinear, but that there are no significant second order effects i.e. parameter interactions. It is worth noting that the overall importance ranking of the main parameters is captured by the correlation methods, with  $q$  showing the highest influence on the output variance as indicated in the discussion of Figure 1. In addition, the use of the Pearson coefficient allows interpretation of the overall sign of the linear response and so aids the physical interpretation of the results. For this reason, the Pearson coefficient is used in the cross-sectional analysis within this paper. However, it should be pointed out that if the nonlinear response is required in any part of the model domain it can be provided by the HDMR component functions at each specific point.

Figure 2 shows the un-normalised TKE Pearson coefficient cross-sections for  $q=90 \pm 10^\circ$  for each input parameter. The surface roughness length has a strong influence on TKE close to the surface grid points, but its influence does not extend very far into the canyon above. The slight negative influence on TKE at the leeward wall surface is due to the lower wind speeds at the surface that occur for higher surface roughness. The wall roughness length has a strong positive effect on TKE for the boundary grid points above roofs and on the windward facing wall, due to application of the log law (1) and boundary condition (2). This positive influence on TKE near the windward wall is accompanied by a negative effect on the mean wind speeds (Table 1) within the canyon as more of the mean kinetic energy is converted into TKE. The effect of inflow roughness on TKE is dominant above the roofs, but extends into the upper part of the canyon. Its relative influence is high in the region where the coefficient for wall roughness changes sign. This sensitivity to inflow boundary conditions may not be considered as a positive feature of the model since it may indicate the need for a larger upwind model domain. However, the low overall variance of the model results suggests that the absolute effect of its input uncertainties may not be particularly large.

## CONCLUSIONS

Cross-sections of output sensitivities to model input parameters show them to be highly location dependant. This indicates that for comparisons with field data, it is important to accurately place buildings and measurement points in the model to get the best approximation of the full scale situation. If a measurement point is close to a surface boundary, the results are very dependant on the correct use of the boundary conditions. Overall it is  $q$  that determines which surfaces are encountered and so over large wind angle changes it usually

has the largest magnitude effect on the model output. This suggests that accurate specification of the background wind direction using an appropriate reference point is required in order to accurately model in canyon flow and turbulence for a particular model scenario.

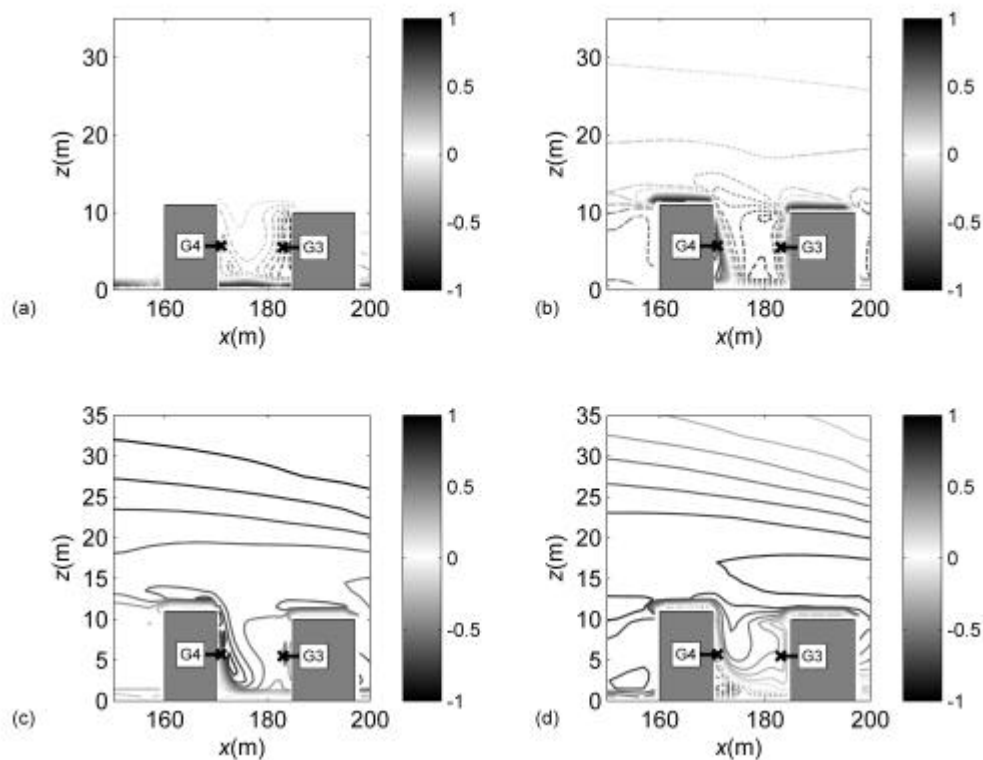


Fig. 2; TKE Pearson correlation coefficient cross section at  $q=90 \pm 10$  degrees for input parameters; (a) surface roughness length, (b) wall and roof roughness length, (c) inflow roughness length, (d) wind direction. Dashed lines indicate negative correlation coefficients.

## REFERENCES

- Benson, J. F., Dixon, N. S., Zeihn T. and A. S. Tomlin, 2007: Global sensitivity analysis of a 3D street canyon model – Part II: Application and physical insight using sensitivity analysis. In preparation.
- Boddy, J. W. D., R. J. Smalley, N. S. Dixon, J. E. Tate, A. S. Tomlin, 2005a: The spatial variability in concentrations of a traffic-related pollutant in two street canyons in York - Part I: The influence of background winds. *Atmos. Environ.*, **39**, 3147-3161.
- Boddy, J. W. D., R. J. Smalley, P. S. Goodman, J. E. Tate, M. C. Bell, and A. S. Tomlin, 2005b: The spatial variability in concentrations of a traffic-related pollutant in two street canyons in York - Part II: The influence of traffic characteristics. *Atmos. Environ.*, **39**, 3163-3176.
- Dixon, N. S., J. W. D. Boddy, R. J. Smalley, and A. S. Tomlin, 2006: Evaluation of a turbulent flow and dispersion model in a typical street canyon in York, UK. *Atmos. Environ.*, **40**, 958-972.
- Eichhorn, J., 1996: Validation of a microscale pollution dispersal model. *Air Pollution Modelling and Its Application XI*, Plenum Publishing Corporation, 539-548.
- Rabitz, H., Ali, O. F., Shorter, J., Shim, K., 1999: Efficient input-output model representations. *Computer Physics communications*, **117**, 11-20.
- Ziehn, T., Tomlin, A. S., 2007: Efficient methods for assessing uncertainties and sensitivities in environmental models. *Proceedings of the 11<sup>th</sup> International Conference on Harmonisation within Atmospheric Dispersion Modeling for Regulatory Purposes*.